Published in final edited form as:
Hepatology. 2009 March ; 49(3): 911–919. doi:10.1002/hep.22708.

Deficiency of NAD(P)H oxidase enhances hepatocellular injury but attenuates fibrosis after chronic carbon tetrachloride administration

Ghazaleh Aram[1], **James J. Potter**[1], **Xiaopu Liu**[1], **Lan Wang**[1], **Michael S. Torbenson**[2], and **Esteban Mezey**[1]

Ghazaleh Aram: ghazaleharam@hotmail.com; James J. Potter: jpotter@jhmi.edu; Xiaopu Liu: xliu32@jhmi.edu; Michael S. Torbenson: mtorben@jhmi.edu; Esteban Mezey: emezey@jhmi.edu

[1]Departments of Medicine, The Johns Hopkins University School of Medicine, Baltimore, Maryland 21205-2195.

[2]Department of Pathology, The Johns Hopkins University School of Medicine, Baltimore, Maryland 21205-2195.

Abstract

Reactive oxygen species (ROS) activate hepatic stellate cells and enhance fibrogenesis. This study determine the role of NAD(P)H oxidase deficiency in the development of hepatocellular necrosis, inflammation and apoptosis in relation to fibrosis produced by chronic CCl_4 administration. Wild-type (WT) mice or mice with deficiency of the gp91^{phox} subunit of NAD(P)H complex (gp91$^{phox-/-}$) were subjected to biweekly CCl_4 injections over 8 weeks, while controls were given isovolumetric injections of olive oil. Serum aspartate aminotransferase (AST) was higher after CCl_4 administration in gp91$^{phox-/-}$ than in WT mice, correlating with increased necrosis on liver histology. By contrast more hepatocyte apoptosis was found after CCl_4 in the WT than in the gp91$^{phox-/-}$ mice, which was associated with changes in components of the mitochondrial pathway of apoptosis, namely an increase in the pro-apoptotic BAX protein in the WT, but not in the gp91$^{phox-/-}$ mice and also a lower cytosolic cytochrome c in the gp91$^{phox-/-}$ mice. There were fewer stellate cells and less fibrosis after CCl_4 in the gp91$^{phox-/-}$ as compared to the WT mice. The increase in α_1(I) collagen mRNA however was greater after CCl_4 in the gp91$^{phox-/-}$ mice. Matrix metalloproteinase-2 (MMP-2) and MMP-9 mRNA increased more in the gp91$^{phox-/-}$ than in WT mice after CCl_4. Tissue inhibitor of metalloproteinase 1 (TIMP-1) and TIMP-2 increased after CCl_4 only in the gp91$^{phox-/-}$ mice.

Conclusions—Decreased hepatic fibrosis after chronic CCl_4 administration in mice with NAD(P)H oxidase deficiency occurs in the setting of greater necrosis and inflammation but decreased apoptosis.

Keywords

Stellate cells; collagen; matrix metalloproteinases; necrosis; apoptosis

Reactive oxygen species (ROS) activate stellate cells and stimulate fibrogenesis (1). Lipid peroxidation products stimulate α_1(I) collagen expression and collagen synthesis by stellate cells in culture (2,3). NAD(P)H oxidase, which generates superoxide ion ($O_2^{\bullet-}$) from oxygen (O_2), is a principal source of ROS. Platelet derived growth factor (PDGF) induced

Please address all correspondence to: Esteban Mezey, M.D., 921 Ross Research Building, The Johns Hopkins University School of Medicine, 720 Rutland Avenue, Baltimore, MD 21205-2195. Telephone: 410-955-7856; FAX: 410-955-9677. E-mail: emezey@jhmi.edu.

proliferation of hepatic stellate cells, which is mediated by ROS produced by NAD(P)H oxidase, was abrogated by inhibition of NAD(P)H with diphenylene iodonium (DPI) pretreatment (4). Furthermore, hepatic fibrosis produced *in vivo* by dimethylnitrosamine was eliminated by daily DPI administration (4). Liver cell death due to necrosis or apoptosis results in inflammatory responses and in fibrogenesis (5,6). Mice with deficiency of the $p47^{phox}$ subunit of NAD(P)H oxidase complex developed less hepatic necrosis and fibrosis after bile duct ligation than wild-type (WT) mice (7). In another study, using a pan-caspase inhibitor, hepatocyte apoptosis, was found to be critical for the development of liver inflammation and fibrosis after bile duct ligation (8). In prior studies, we found that mice with NAD(P)H oxidase deficiency, due to lack of the $gp91^{phox-/-}$ subunit of NAD(P)H complex ($gp91^{phox-/-}$), developed less hepatic fibrosis after chronic CCl_4 administration than WT mice (9), but the means of cell death were not assessed. In a more recent study, $gp91^{phox-/-}$ and WT mice fed a methionine and choline deficient diet for 8 weeks developed similar amounts of necroinflammatory change and fibrosis (10).

The purpose of this study was to determine how NAD(P)H oxidase deficiency decreases hepatic fibrosis produced by chronic CCl_4 administration by examining the roles of hepatocellular necrosis, inflammation and apoptosis.

MATERIALS & METHODS

Animals and Materials

Male wild-type (WT) C57BL/6J and $gp91^{phox-/-}$ mice were purchased from Jackson Laboratory (Bar Harbor, ME). All animals received humane care in compliance with the guidelines from the Animal Care and Use Committee of The Johns Hopkins University. Sirius Red was obtained from Polysciences, Inc, Warrington, PA. Carbon tetrachloride (CCl_4) and goat anti-mouse α-smooth muscle actin Cy3 conjugate antibody were purchased from Sigma Chemical Co., St. Louis, MO. Caspase 3 and Caspase 8 fluorometric assay kits were obtained from BioVision (Mountain View, CA)

Animal treatment

Mice at 4–6 weeks of age weighing 20–30g were kept in a temperature-controlled room with an alternating 12-h dark and light cycle. Eight WT and 8 $gp91^{phox-/-}$ mice were given intraperitoneal (i.p) injections of CCl_4 biweekly as 5 μl of a 20% solution of CCl_4 in olive oil per g body weight (1.0 ml/kg of CCl_4). The 8 control WT and 8 $gp91^{phox-/-}$ mice received the same isovolumetric dose of olive oil as i.p. injections. The animals were sacrificed at one week and at 8 weeks after the start of the injections. At the time of sacrifice, blood was obtained from the aorta for measurements of aminotransferases and the samples were stored at −20°C. The liver was removed, rinsed with phosphate buffered saline (PBS), and divided into four portions: (a) fixed in 10% buffered formaldehyde formalin and embedded in paraffin; (b) snap frozen at −70°C for sectioning and immunohistochemistry; (c) homogenized in appropriate buffer(s) and aliquots of the homogenates or the separated cytosols after centrifugation frozen at −70°C for biochemical assays; and (d) placed in RNA STAT-60 solution (from Tel-Test, Inc, Friendswood, TX) and stored in −70°C for RNA isolation.

Liver histology and morphometric collagen determination

The liver sections imbedded in paraffin were cut (5μ) and stained with hematoxylin-eosin (H&E), Masson's trichrome, or sirius red. The extent of necrosis and inflammation was evaluated on blinded slides by M.S.T. from our Department of Pathology. Fibrosis was determined histologically by measuring the intensity of fibrosis in four to six (x 100) digital images captured from slides of each mouse stained with sirius red. The total fibrosis density

score was determined by dividing the image intensity by the image area as described previously (11).

Quantitation of stellate cells

Immunofluorescent staining for α-smooth muscle actin (α -SMA) was done in deparaffinized liver sections. The slides were washed in deionized water for 1 min and in PBS for 5 min, followed by blocking using PBS-5% FBS. The slides were incubated with Cy3 conjugated monoclonal α -SMA antibody (Sigma, 1:500 in PBS-5% FBS) for 1 h at room temperature and subsequently at 4°C overnight. After washing with PBS 4 times for 15 min, the slides were mounted and 8 areas per slide captured by fluorescent microscopy (magnification x100). Stellate cells were counted in 8 fields per slide for each mouse.

Serum Aminotransferases

Alanine aminotransferase (ALT) and aspartate aminotransferase (AST) were determined by the spectrophotometric method of Bergmeyer et al. (12).

Mitochondrial ATP

Liver mitochondria were isolated by differential centrifugation from liver homogenates as described previously (13). ATP was determined with a Bioluminescent Assay Kit obtained from Sigma Chemical Company. Mitochondrial protein was determined by the method of Lowry et al (14)

Liver malondialdehyde

Liver slices were homogenized with cold 1.15% KCl and malondialdehyde was determined using thiobarbituric acid by the method of Uchiyama and Mihara (15).

Determination of messenger RNA by real time quantitative polymerase chain reaction RT-qPCR

The 7900 HT (Applied Biosystems, Foster City, CA) and the SDS 2.2.1 software was used to perform RT-qPCR at the The Johns Hopkins DNA Analysis Facility. Total cellular RNA from a portion of liver was placed in RNA STAT 60 reagent and following their protocol, RNA was purified and isolated. The concentration of the isolated RNA was determined from the optical density at 260nm and its purity from the 260nm/280nm OD ratio. The isolated RNA was stored at −80° C. RT-qPCR for α_1(I) collagen mRNA and transforming growth factor-β (TGF-β)were performed using sequence-specific probes from TaqMan gene expression assays of Applied Biosystems (Foster City, CA). Probes for mouse TGF-β 1, α_1(I) collagen, β–actin (as endogenous control), mouse matrix metalloproteinase (MMP) -2 (MMP-2), and MMP-9 were obtained from Applied Biosystems. Superscript III first strand synthesis from Invitrogen (Carlsbad, CA) was used to synthesize first strand cDNA from the purified RNA. Gene-transcript levels of the above probes were compared to β-actin, the housekeeping endogenous control. Variation in the amount of the transcripts was corrected by the level of expression of the β-actin gene in each individual sample.

Western Blot Analysis

Liver sections were homogenized in 50 mM Tris-HCl buffer pH 7.6 containing 150 mM NaCl, 10 mM $CaCl_2$, 0.25% Triton-X, 0.1 μM phenylmethanesulfonyl fluoride (PMSF), 10 μM leupetin, 10 μM pepstatin, 0.1 mM iodoacetamide and 25 μg aprotonin and then centrifuged at 9,000g for 10 min at 4°C. The cytosol protein in the supernatant was initially stored at −80°C. The proteins were separated on mini-SDS gels at 100 V for 1 h and electrotransferred to nitrocellulose transblot membranes (BioRad, Hercules, CA). The membranes were washed in PBS, pH 7.6, containing 0.1% Tween 20 (PBS-T), blocked with

5% (W/V) dry nonfat milk in PBS-T for 1 h, rinsed with PBS-T and then incubated with either rabbit anti-mouse antibodies to Fas, Bax, BclXs/l, Bcl-2, cytochrome c, MMP-2, MMP-9, TIMP-1, TIMP-2 or β actin, obtained from Santa Cruz Biotechnology, Inc, Santa Cruz, CA. After repeated washing, the membranes were incubated with horseradish peroxidase-conjugated goat anti-rabbit IgG (1:10,000 dilution; Amersham Biosciences, Piscataway, NJ) at room temperature for 1 h. The membranes were then washed again and visualized by enhanced chemiluminescence reaction (ECL Plus; Amersham Biosciences). Densitometry was determined using Image J v 1.30 obtained from NIH.

Terminal Deoxynucleotidyl Transferase-Mediated Nick-End Labeling Assay

Terminal deoxynucleotidyl transferase-mediated nick-end labeling (TUNEL) assay was performed on paraffin embedded liver slices with the cell death detection kit from Roche Applied Science (Nutley, NJ). Fluorescence microscope using the FITC filter revealed the apoptotic bodies which were counted.

Apoptosis in stellate cells

Apoptosis in stellate cells was determined in ultrathin liver slices by formamide-induced DNA denaturation with detection of single stranded DNA (ssDNA) described by Frankfurt and Krishan (16), with mouse monoclonal antibodies to ssDNA (Millipore, Temecula, CA) and anti-mouse IgG (whole molecule) FITC as secondary antibody (Sigma). The immunostained slices were evaluated and photographed with laser confocal microscopy.

Caspase activities

The activities of caspase 3 and caspase 8 were determined in liver homogenates by measuring proteolytic cleavage of the specific fluorogenic substrates, DEVD-AFC and IETD-AFC (AFC: 7-amino-4-trifluoromethyl coumarin) respectively BioVision). The results are expressed as relative units per milligram of protein.

Statistical Analysis

In most measurements, the mean and the standard error of the mean were calculated. The data was analyzed with the Student's *t* test or by two way analysis of variance (ANOVA) when comparing means of more than two groups.

RESULTS

Liver injury and fibrosis

The morphological changes of liver injury and fibrosis caused by CCl_4 were visualized in sections stained by H&E (not shown) and sirius red. The changes include necrosis, inflammation with macrophages, lymphocytes and fibrosis. Fatty infiltration was minimal. The grades of necroinflammatory changes were higher after CCl_4 in the $gp91^{phox-/-}$ mice as compared to the WT mice ($p<0.05$) (Fig. 1). Liver fibrosis was more evident in the WT than in the $gp91^{phox-/-}$ mice (Fig.2A–B). The area of hepatic fibrosis detected by Sirius red staining and densitometric analysis was significantly higher in the WT mice after CCl_4 as compared to the other mice groups ($p<0.01$) (Fig. 2C) The number of stellate cells, identified by α-smooth muscle actin staining, was lower per x200 field after CCl_4 in the $gp91^{phox-/-}$ mice than in WT mice (Fig 2D). The values were 33.9 ± 2.8 in $gp91^{phox-/-}$ as compared to 50.0 ± 4.8 in the WT mice ($p<0.05$).

Serum aminotransferases were elevated after CCl_4 administration (Fig.1). The increase of AST was higher in $gp91^{phox-/-}$ than in WT mice ($p<0.05$). By contrast, ALT was not significantly different in the $gp91^{phox-/-}$ than in the WT mice.

The increase in α_1(I) collagen mRNA after CCl_4 administration was greater in the gp91$^{phox-/-}$ than in the WT mice ($p<0.05$) (Fig. 3). The increase in TGFβ mRNA was also greater in the gp91$^{phox-/-}$ than in the WT mice ($p<0.05$) (Fig. 3). However, TGFβ protein on Western blot analysis was not significantly changed by CCl_4 in either group of mice (data not shown).

Liver malondialdehyde was markedly increased in the WT mice after CCl_4 administration from a control value of 9.4 ± 1.4 to 19.1 ± 1.5 μmoles/g liver ($p<0.01$). In the gp91$^{phox-/-}$ animals, liver malondialdehyde increased from 5.8 ± 1.8 to 10.3 ± 0.2 ($p<0.05$).

Apoptosis

The number of apoptotic hepatocytes was highest in the WT mice after CCl_4 administration (Fig. 4B). The values from 40–100 fields (x100) examined were 1.63 ± 0.42 and 1.67 ± 0.43 apoptotic cells per field for WT and gp91$^{phox-/-}$ controls respectively and 69.2 ± 4.05 and 14.93 ± 2.17 for WT and gp91$^{phox-/-}$ after CCl_4 administration ($p<0.01$).

Fas (CD95/APO-1) receptor mediates apoptosis principally via the extrinsic death receptor pathway. Two Fas receptor proteins were detected by western blot in livers of the mice. CCl_4 did not result in significant changes in Fas receptor proteins in the WT or gp91$^{phox-/-}$ mice (Fig.5A). Activated caspases 3 and 8 are essential in the extrinsic death receptor pathway of apoptosis. Caspase 3 was increased to a greater extent in the gp91$^{phox-/-}$ mice than the WT mice after CCl_4 administration ($p<0.05$) (Fig. 5B), while the increase in Caspase 8 was similar after CCl_4 in the gp91$^{phox-/-}$ and WT mice. Components of the mitochondrial pathway of apoptosis that respond to intracellular stress signals were examined. Pro-apoptotic BAX protein was increased after CCl_4 in the WT, but not in the gp91$^{phox-/-}$ mice ($p<0.01$) (Fig.6), while BclX $_{S/L}$ was not affected by CCl_4 administration in either the gp91$^{phox-/-}$ or WT mice (Fig.6). The anti-apoptotic protein Bcl-2 decreased after CCl_4 in the gp91$^{phox-/-}$ ($p<0.01$) but not in the WT mice (Fig.6). Cytosolic cytochrome c, which is released from the mitochondria during apoptosis and is regulated by both pro- and anti-apoptotic members of the Bcl-2 family of proteins, was decreased after CCl_4 in the gp91$^{phox-/-}$ CCl_4 group ($p<0.05$), but not in the WT mice (Fig. 6).

Stellate cell apoptosis, evaluated by the presence of ssDNA under confocal microscopy, was not detected in the gp91$^{phox-/-}$ or the WT mice after CCl_4 (data not shown).

Matrix metalloproteinases

Liver matrix metalloproteinase-2 (MMP-2) was increased after CCl_4 in the WT mice ($p<0.05$) but not in the gp91$^{phox-/-}$ mice (Fig.7), while matrix metalloproteinase 9 (MMP-9) was not changed by CCl_4 in either group of mice (Fig.7). Increases in MMP-2 mRNA and in MMP-9 mRNA were greater after CCl_4 in the gp91$^{phox-/-}$ than in the WT mice. The increase in MMP-2 mRNA after CCl4 was 30 fold in the gp91$^{phox-/-}$ mice as compared to 7 fold in the WT mice ($p<0.01$), while the increase in MMP-9 mRNA was 111 fold in the gp91$^{phox-/-}$ mice as compared to 5 fold in the WT mice ($p<0.01$) (data not shown).

Tissue inhibitor of metalloproteinase 1 (TIMP-1) (Fig. 7) and TIMP-2 were lower in the control WT than in the control gp91$^{phox-/-}$ mice (Fig.10). After CCl_4, both TIMP-1 and TIMP-2 increased only in the WT mice ($p<0.05$) to levels similar to those found in the control or CCl_4 treated gp91$^{phox-/-}$ mice (Fig. 7).

Effects of administration of CCl_4 for one week

The effects of acute CCl_4 on hepatic injury and fibrosis were determined in a separate experiment. After one week CCl_4 administration the grade of necrosis, but not of

inflammatory changes, was higher in the WT mice than in gp91$^{phox-/-}$ mice ($p<0.05$) (Fig. 8). Liver fibrosis detected by sirius red staining was minimal and similar in the WT than in the gp91$^{phox-/-}$ mice (not shown). Also the number of stellate cells, identified by α-smooth muscle actin staining, was similar per x200 field after CCl_4 in the gp91$^{phox-/-}$ mice than in WT mice. The values were 9.8 ± 1.6 and 9.3 ± 0.7 in gp91$^{phox-/-}$ and the WT mice respectively. The increase of serum ALT was higher in WT ($p<0.01$) than in gp91^{phox} mice ($p<0.05$) (Fig. 8). By contrast, AST was not significantly different in the gp91$^{phox-/-}$ than in the WT mice.

The number of apoptotic hepatocytes was similar in the WT than in gp91$^{phox-/-}$ mice after CCl_4 administration. The values from 32 fields (x100) examined were 1.2 ± 0.5 and 1.2 ± 0.4 apoptotic cells per field for WT and gp91$^{phox-/-}$ controls respectively and 12.4 ± 1.7 and 8.9 ± 1.5 for WT and gp91$^{phox-/-}$ after CCl_4 administration. Caspase 3 was increased in the gp91$^{phox-/-}$ mice but not the WT mice, while caspase 8 was unchanged in both groups of mice (Fig. 9A) Cytosolic cytochrome c was increased, while mitochondrial cytochrome c was decreased, after CCl_4 in the WT mice ($p<0.05$), while no significant changes occurred in the gp91$^{phox-/-}$ (Fig. 9B). There was a mean 31% decrease in mitochondrial ATP after CCl_4 in the WT mice, and an opposite 34% increase in the gp91$^{phox-/-}$, however these changes were not statistically significant. The values for 8 mice in each group were 16.4 ± 3.9 and 11.3 ± 1.7 nmoles/mg protein for WT mice, compared to 9.5 ± 1.8 and 12.7 ± 2.6 nmoles/mg protein for gp91$^{phox-/-}$ before and after CCl_4 respectively.

The increase in α_1(I) collagen mRNA after CCl_4 administration was greater in the gp91$^{phox-/-}$ than in the WT mice ($p<0.05$) (Fig.10) and TGFβ mRNA was increased in the gp91$^{phox-/-}$ but not in the WT mice ($p<0.05$) (Fig.10). MMP-2 mRNA and in MMP-9 mRNA increased after CCl_4 in the gp91$^{phox-/-}$ but not in the WT mice. TIMP-1 mRNA increased to as greater extent in the gp91$^{phox-/-}$ than in the WT mice (Table 1). MMP-2 and MMP-9 proteins were not changed significantly after 1 week of CCl_4 in either the WT or the gp91$^{phox-/-}$ mice (Fig.11). TIMP-1 protein decreased after CCl_4 in the gp91$^{phox-/-}$ mice but not in the WT mice, while TIMP2 decreased in the WT mice remaining unchanged in the gp91$^{phox-/-}$ mice (Fig. 11).

DISCUSSION

The development of less hepatic fibrosis after chronic CCl_4 administration in the gp91phox$^{-/-}$ mice than in WT mice in this study was associated with greater hepatocellular necrosis and inflammation but with decreased hepatocyte apoptosis. The higher serum AST in the gp91$^{phox-/-}$ mice, which correlated with the greater hepatocellular necrosis and inflammation, is consistent with enhanced mitochondrial injury, since approximately 80% of the AST is found in mitochondria, while ALT is found in the cytosol (17). Our results of greater hepatocellular necrosis and inflammation in the gp91$^{phox-/-}$ mice differ from the findings of other studies using different means to produce liver injury and/or fibrosis. Steatosis, inflammation and necrosis were observed in WT, but not in NAD(P)H oxidase deficient mice given chronic ethanol administration (18), however the effect on fibrosis was not assessed in that study because no significant fibrosis occurred. Our study also shows that the short term administration of CCl_4 ,which does not result in significant increase in fibrosis, results in greater hepatocellular necrosis and higher serum ALT in the WT than in the gp91$^{phox-/-}$ mice.

The development of less hepatic fibrosis after bile duct ligation in mice with deficiency of the p47^{phox} subunit of NAD(P)H oxidase complex than in WT mice was associated with lower elevations of serum AST, and less necrosis around the biliary tracts (7). Hepatocyte apoptosis, which was not determined in the above study, has since been demonstrated to be

critical for the development of liver inflammation and fibrosis after bile duct ligation (8). In another study, gp91$^{phox-/-}$ and WT mice fed a methionine and choline deficient diet developed similar amounts of necroinflammatory change and fibrosis (10). The mechanism for the decreased apoptosis after CCl_4 in the gp91phox$^{-/-}$ mice is most likely due to a decrease in the mitochondrial pathway of apoptosis. The pro-apoptotic protein BAX protein, which was increased in the WT mice, remained unchanged in the gp91$^{phox-/-}$ mice, while cytosolic cytochrome c, which is released from the mitochondria during apoptosis was decreased after CCl_4 in the gp91$^{phox-/-}$ mice. Of note is that one week after CCl_4 administration there was a marked increase in cytosolic cytochrome c in association with a decrease in mitochondrial cytochrome c in the WT but not in the gp91$^{phox-/-}$ mice CCl_4. These changes are most likely a reflection of the more severe hepatocellular injury in the WT mice. The increase in cytosolic cytochrome probably predisposes to increased apoptosis in the WT mice, although no differences in apoptosis were observed between WT and gp91$^{phox-/-}$ mice at one week. The Fas (CD95/APO-1) receptor which mediates apoptosis caused by a variety of insults (19), principally via the extrinsic death receptor pathway, was not changed significantly by chronic CCl_4 administration in either the WT or the gp91$^{phox-/-}$ mice. Activated caspases 3 and 8, are also essential in the extrinsic death receptor pathway of apoptosis. Caspase 3 was increased to as greater extent in the gp91$^{phox-/-}$ mice than in the WT mice after CCl_4 administration, while the increases in Caspase 8 were similar after CCl_4 in both groups of mice. An increase in caspase 3 in the gp91$^{phox-/-}$ but not the WT mice was already evident after one week of CCl_4 administration. The significance of the greater increase in caspase 3 in the gp91$^{phox-/-}$ mice than in the WT mice, in relation to the lesser increase in apoptosis after CCl_4 in the gp91$^{phox-/-}$ mice, is unknown.

The decrease in apoptosis in the gp91$^{phox-/-}$ mice as compared to the WT mice after chronic CCl_4 is most likely due to decreased ROS generation. Previous studies have shown that TGFβ induced apoptosis of fetal rat hepatocytes requires ROS generation, mitochondrial permeability transition with cytochome c release, and caspase activation (20). Furthermore, blockage of the TGFβ induced increase in ROS by DPI, which inhibits NAD(P)H oxidase and other flavoproteins, abrogated the effect of TGFβ on increasing apoptosis (18). Also, relating to the role of NAD(P)H oxidase, it has been observed that neutrophils exposed to stress stimuli from patients with chronic granulomatous disease, which are deficient in NAD(P)H oxidase, show decreased apoptosis as compared to neutrophis from normal subjects (21). Furthermore, apoptosis induced acutely by bile salt in cultured rat hepatocytes was blunted by inhibition of NAD(P)H oxidase (22). Increased apoptosis of hepatocytes with phagocytosis of apoptotic bodies by Kuppfer and stellate cells has been linked to fibrogenesis (6). On the other hand, apoptosis of stellate cells was shown to contribute to the resolution of fibrosis after discontinuation of chronic CCl_4 administration in rats (23). In our study, apoptosis was not demonstrated in stellate cells from either gp91$^{phox-/-}$ or WT mice after CCl_4 administration.

As relates to the mechanism for the decreased hepatic fibrosis after chronic CCl_4 administration in the gp91$^{phox-/-}$ as compared to the WT mice, changes in both collagen formation and degradation were considered. The greater increase in the α_1(I) collagen mRNA in the gp91$^{phox-/-}$ mice than in the WT mice, found after 1 and 8 weeks of CCl_4 administration, indicates that NAD(P)H deficiency does not decrease collagen formation.. Furthermore, TGFβ mRNA was also higher in the gp91$^{phox-/-}$ mice than in the WT mice. This observation agrees with prior findings indicating that TGFβ transcription is negatively regulated by NAD(P)H oxidase mediated oxygen radicals (24). In our study, however, the greater increase in TGFβ mRNA in the gp91$^{phox-/-}$ mice than in the WT mice was not accompanied by changes in TGFβ protein. Post-translational changes, such as feedback inhibition by procollagen propeptides, may be a factor for the lower accumulation of

collagen in the gp91$^{phox-/-}$ mice after CCl_4 in the setting of increased α_1(I) collagen mRNA. However, while this was shown in cultured stellate cells from normal rats, it was not found in stellate cells isolated from fibrotic livers (25). It is well established that ROS activate stellate cells and stimulate fibrogenesis (1). In our study the lesser accumulation in malondialdehyde, a product of lipid peroxidation, after CCl_4 in the gp91$^{phox-/-}$ was associated with lower collagen deposition, indicating lower but not absent ROS formation from other sources most likely the mitochondria. It is well known that chronic CCl_4 administration impairs the mitochondrial electron transport chain and that this is associated with increased formation of ROS (26–28). There is evidence in this study that increased collagen degradation contributes to the lesser accumulation of hepatic fibrosis in gp91$^{phox-/-}$ mice. Increased collagen formation from CCl_4 administration (29,30) and from other insults (31) is associated with an increase in collagen degradation. Indeed, in this study, the increases in MMP-2 mRNA and MMP-9 mRNA were greater after one and 8 weeks of CCl_4 in the gp91$^{phox-/-}$ than in the WT mice. However, this was not accompanied by higher MMP-2 and MMP-9 protein levels. More importantly, TIMP-1 and TIMP-2 proteins increased after chronic CCl_4 administration in the WT mice but not in the gp91$^{phox-/-}$ mice. TIMPs inhibit secretion and activation of metalloproteinases, hence inhibiting collagen degradation (32). In conclusion, this study shows decreased hepatic fibrosis after chronic CCl_4 administration in NAD(P)H oxidase deficient mice as compared to WT mice in association with greater hepatocellular necrosis and inflammation but decreased hepatocyte apoptosis. The lower hepatic fibrosis was found in the setting of a lower number of stellate cells, a greater increase in α_1(I) collagen mRNA, but a lack of an increase in TIMP in the NAD(P)H deficient mice as compared to the WT mice, suggesting that NAD(P)H deficient mice have enhanced degradation of the formed collagen.

Abbreviations

ROS	reactive oxygen species
CCl_4	carbon tetrachloride
WT	wild type
gp91$^{phox-/-}$	glycoprotein subunit 91 NADPH oxidase deficient mice
AST	aspartate aminotransferase
MMP	matrix metalloproteinase
TIMP	tissue inhibitor metalloproteinase
PDGF	platelet derived growth factor
DPI	diphenylene iodonium
PBS	phosphate buffered saline
FBS	fetal bovine serum
H&E	hematoxylin-eosin
α-SMA	α -smooth muscle actin
ALT	alanine aminotransferase
RT-qPCR	real time quantitative polymerase chain reaction
TGF-β	transforming growth factor-β
PMSF	phenylmethanesulfonyl fluoride
TUNEL	terminal deoxynucleotidyl transferase-mediated in situ end labeling

Acknowledgments

Financial support

This work was supported by Grant AA000626 from the United States Public Health Service. G.A. is a postdoctoral fellow on National Research Service Award 2 T32 AA07467 from the National Institute of Alcohol Abuse and Alcoholism (NIH). The authors acknowledge assistance from The Hopkins Digestive Diseases Basic Research Development Center (NIH grant 2464388) in the performance of this study.

REFERENCES

1. Nieto N, Friedman SL, Greenwel P, Cederbaum AI. CYP2E1-mediated oxidative stress induces collagen type I expression in rat hepatic stellate cells. Hepatology. 1999; 30:987–996. [PubMed: 10498651]
2. Chojkier M, Houglum K, Solis-Herruzo J, Brenner DA. Stimulation of collagen gene expression by ascorbic acid in cultured human fibroblasts. A role for lipid peroxidation? J Biol Chem. 1989; 264:16957–16962. [PubMed: 2777815]
3. Maher JJ, Tzagarakis C, Gimenez A. Malondialdehyde stimulates collagen production by hepatic lipocytes only upon activation in primary culture. Alcohol Alcohol. 1994; 29:605–610. [PubMed: 7811345]
4. Adachi T, Togashi H, Suzuki A, Kasai S, Ito I, Sugahara K, et al. NAD(P)H oxidase plays a crucial role in PDGF-induced proliferation of hepatic stellate cells. Hepatology. 2005; 41:1272–1281. [PubMed: 15915457]
5. Canbay A, Friedman S, Gores GJ. Apoptosis: the nexus of liver injury and fibrosis. Hepatology. 2004; 39:273–278. [PubMed: 14767974]
6. Malhi H, Gores GJ, Lemasters JJ. Apoptosis and necrosis in the liver: A tale of two deaths? Hepatology. 2006; 43:S31–S44. [PubMed: 16447272]
7. Bataller R, Schwabe RF, Choi YH, Yang L, Paik YH, Lindquist J, et al. NADPH oxidase signal transduces angiotensin II in hepatic stellate cells and is critical in hepatic fibrosis. J Clin Invest. 2003; 112:1383–1394. [PubMed: 14597764]
8. Canbay A, Feldstein A, Baskin-Bey E, Bonk SF, Gores GJ. The caspase inhibitor IND-6556 attenuates hepatic injury and fibrosis in the bile duct ligated mouse. J Pharmacol Exp Ther. 2004; 308:1191–1196. [PubMed: 14617689]
9. Novitskiy G, Potter JJ, Wang L, Mezey E. Influences of reactive oxygen species and nitric oxide on hepatic fibrogenesis. Liver Int. 2006; 26:1248–1257. [PubMed: 17105591]
10. dela Pena A, Leclercq IA, Williams J, Farrell GC. NADPH oxidase is not an essential mediator of oxidative stress or liver injury in murine MCD diet-induced steatohepatitis. J Hepatol. 2007; 46:304–313. [PubMed: 17157947]
11. Potter JJ, Rennie-Tankersley L, Mezey E. Influence of leptin in the development of hepatic fibrosis produced in mice by *Schistosoma mansoni* infection and by chronic carbon tetrachloride administration. J Hepatol. 2003; 38:281–288. [PubMed: 12586293]
12. Bergmeyer HU, Scheibe P, Wahlefeld AW. Optimization of methods for aspartate aminotransferase and alanine aminotransferase. Clin Chem. 1978; 24:58–73. [PubMed: 22409]
13. Reed WD, Mezey E. Effects of chronic ethanol feeding on enzymes of rat brain and liver mitochondria. Life Sci. 1972; 11:847–857.
14. Lowry OH, Rosebrough NJ, Farr AL, Randall RJ. Protein measurement with the folin phenol reagent. J. Biol. Chem. 1951; 193:265–275. [PubMed: 14907713]
15. Uchiyama M, Mihara M. Determination of malondialdehyde precursor in tissues by thiobarbituric acid test. Anal Biochem. 1978; 86:271–278. [PubMed: 655387]
16. Frankfurt OS, Krishan A. Identification of apoptotic cells by formamide-induced DNA denaturation in condensed chromatin. J Histochem Cytochem. 2001; 49:369–378. [PubMed: 11181740]
17. Rej R. Aspartate aminotransferase activity and isoenzyme proportions in human liver tissues. Clin Chem. 1978; 24:1971–1979. [PubMed: 213206]

18. Kono H, Rusyn I, Yin M, Gabele E, Yamashina S, Dikalova A, et al. NADPH oxidase–derived free radicals are key oxidants in alcohol-induced liver disease. J Clin Invest. 2000; 106:867–872. [PubMed: 11018074]
19. Galle PR, Hofmann WJ, Walczak H, Schaller H, Otto G, Stremmel W, et al. Involvement of the CD95 (APO-1/Fas) receptor and ligand in liver damage. J Exp Med. 1995; 182:1223–1230. [PubMed: 7595193]
20. Herrera B, Murillo MM, Alvarez-Barrientos A, Beltran J, Fernandez M, Fabregat I. Source of early reactive oxygen species in the apoptosis induced by transforming growth factor- β in fetal rat hepatocytes. Free Radic Biol Med. 2004; 36:16–26. [PubMed: 14732287]
21. Gardai S, Whitlock BB, Helgason C, Ambruso D, Fadok V, Bratton D, et al. Activation of SHIP by NADPH oxidase-stimulated Lyn leads to enhanced apoptosis in neutrophils. J Biol Chem. 2002; 277:5236–5246. [PubMed: 11724799]
22. Reinehr R, Becker S, Keitel V, Eberle A, Grether-Beck S, Haussinger D. Bile salt-induced apoptosis involves NADPH oxidase isoform activation. Gastroenterology. 2005; 129:2009–2031. [PubMed: 16344068]
23. Iredale JP, Benyon RC, Pickering J, McCullen M, Northrop M, Pawley S, et al. Mechanisms of spontaneous resolution of rat liver fibrosis. Hepatic stellate cell apoptosis and reduced hepatic expression of metalloproteinase inhibitors. J Clin Invest. 1998; 102:538–549. [PubMed: 9691091]
24. Wolf G, Hannken T, Schroeder R, Zahner G, Ziyadeh FN, Stahl RAK. Antioxidant treatment induces transcription and expression of transforming growth factor β in cultured renal proximal tubular cells. FEBS Lett. 2001; 488:154–159. [PubMed: 11163763]
25. Ikeda H, Wu GY, Wu CH. Lipocytes from fibrotic rat liver have an impaired feedback response to. procollagen propeptides. Am J Physiol Gastrointest. Liver Physiol. 1993; 264:G157–G162.
26. Krahenbuhl L, Ledermann M, Lang C, Krahenbuhl S. Relationship between hepatic mitochondrial functions *in vivo* and *in vitro* in rats after carbon tetrachloride-induced liver cirrhosis. J. Hepatol. 2000; 33:216–1223. [PubMed: 10952239]
27. Wang CY, Ma FL, Liu JT, Tian JW, Fu FH. Protective effect of salvianic acid A on acute liver injury induced by carbon tetrachloride in rats. Biol Pharm Bull. 2007; 30:44–47. [PubMed: 17202657]
28. Cadenas E, Davies KJA. Mitochondrial free radical generation, oxidative stress, and aging. Free Radical Biol Med. 2000; 29:222–230. [PubMed: 11035250]
29. Hernandez-Munoz R, Diaz-Munoz M, Suarez-Cuenca JA, Trejo-Solis C, Lopez V, Sanchez-Sevilla L, et al. Adenosine reverses a preestablished CCl_4-induced micronodular cirrhosis through enhancing collagenolytic actrivity and stimulating hepatocyte cell proliferation in rats. Hepatology. 2001; 34:677–687. [PubMed: 11584363]
30. Zhou X, Hovell CJ, Pawley S, Hutchings MI, Arthur MJP, Iredale JP, et al. Expression of matrix metalloproteinase-2 and -14 persists during early resolution of experimental liver fibrosis and might contribute to fibrolysis. Liver Int. 2004; 24:492–501. [PubMed: 15482348]
31. Mezey E, Potter JJ, Slusser RJ, Abdi W. Changes in hepatic collagen metabolism in rats produced by chronic ethanol feeding. Lab Invest. 1977; 36:206–214. [PubMed: 557149]
32. Benyon RC, Arthur MJP. Extracellular matrix degradation and the role of hepatic stellate cells. Semin Liver Dis. 2001; 21:373–384. [PubMed: 11586466]

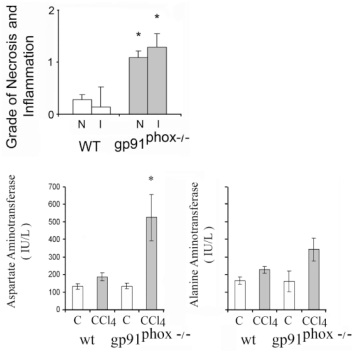

Fig. 1.

Necroinflammatory changes and serum aminotransferases after 8 weeks of chronic carbon tetrachloride (CCl_4) administration in wild type (WT) and gp91$^{phox-/-}$ mice. Liver cell necrosis (N) was evaluated on a scale of 1–4 as follows: 1, occasional; 2, mild scattered; 3, confluent zonal and 4, extensive. Grades for hepatic inflammation (I) were: 1, scattered; 2, mild; 3, moderate and 4, marked. The histological changes were assessed in x 20 magnification fields of slides stained with hematoxylin-eosin (H&E). The values are expressed as means ± SE of 8 determinations per group. *p<0.05 vs. WT for necroinflammatory changes. *p<0.05 vs control for serum aminotransferases.

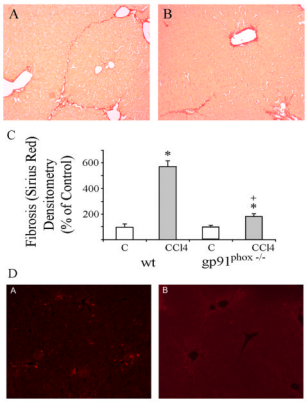

Fig.2.

Histology with sirius red collagen staining of liver sections from (A) WT and (B) $gp91^{phox-/-}$ mice after 8 weeks of chronic CCl_4 administration. (original magnification × 100). C. Relative densitometry of fibrosis in WT and $gp91^{phox-/-}$ mice after chronic CCl_4 administration. The degree of fibrosis was measured by sirius red staining and densitometry of the various groups. The density of fibrosis was determined as intensity of sirius red staining divided by the area of the captured field. A total of 24 fields were captured from livers of each group of mice. The values are expressed as means ± SE. * $p< 0.01$ vs. respective control. $^{+}$ $p<0.01$ vs WT + CCl_4. D. Immunofluorescent detection of activated stellate cells in (A) WT and (B) $gp91^{phox-/-}$ mice after chronic CCl_4 administration. The liver slices were incubated with Cy3 monoclonal α-smooth muscle actin antibody (original magnification × 100).

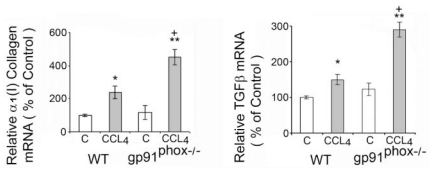

Fig.3.

Liver α_1(I) collagen mRNA and transforming growth factor β (TGFβ) mRNA in WT and gp91$^{phox-/-}$ mice after chronic CCl_4 administration. The mRNAs were determined by real time quantitative PCR. The relative amounts of mRNA were normalized against β-actin in the same samples. The values are expressed as means ± SE of 8 determinations per group. * $p<0.05$ vs. control. ** $p<0.01$ vs. control. + $p<0.05$ vs. WT + CCl_4.

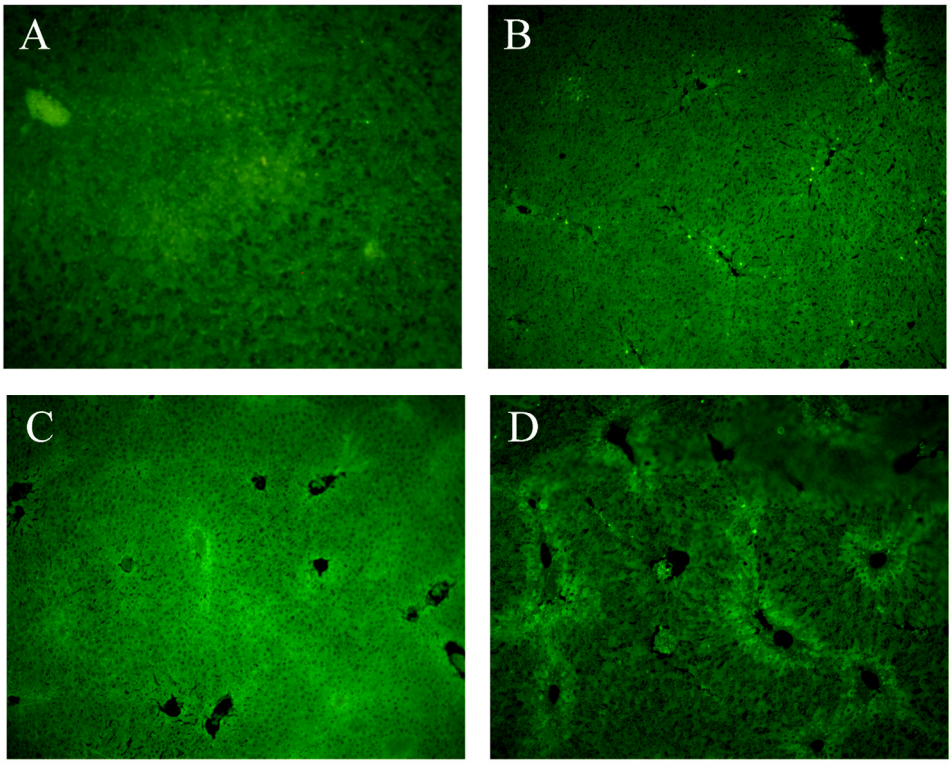

Fig.4.

Apoptosis determined by TUNEL staining of liver sections from WT and gp91$^{phox-/-}$ mice after chronic CCl_4 administration. (A) WT-control; (B) WT + CCl_4; (C) gp91$^{phox-/-}$ control; (D) gp91$^{phox-/-}$ + CCl_4. Original magnification × 100.

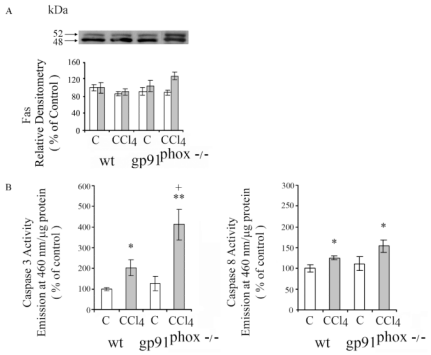

Fig. 5.

Effects of chronic CCl_4 on in WT and gp91$^{phox-/-}$ mice on A. FAS and B. Activities of caspase 3 and 8. FAS was determined by western blot and quantitated by densitometry. White bars represent 52 kDA and shaded bars 48 kDa Fas. All values are expressed as means ± SE of 8 measurements per group.

* $p < 0.05$ vs. respective control. **$p<0.01$ vs.respective control; $^{+}p<0.05$ vs. WT + CCl_4.

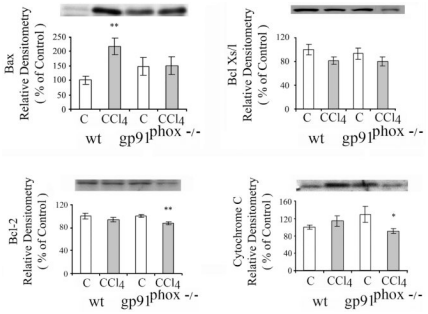

Fig. 6.

Effects of chronic CCl_4 administration on Bax, Bcl Xs/l Bcl-2 and cytosolic cytochome c in WT and $gp91^{phox-/-}$ mice. The determinations were done by western blot. The values are expressed as means ± SE of relative densitometry of 8 measurements per group. * $p< 0.05$ vs. control. **$P<0.01$ vs. control.

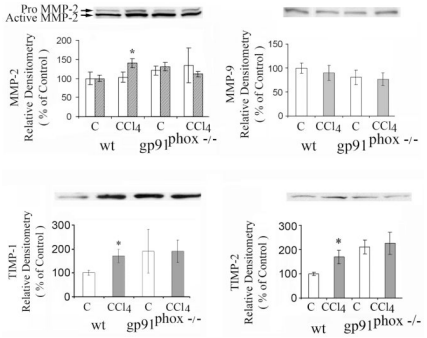

Fig. 7.

Effects of chronic CCl_4 administration on matrix metalloproteinase 2 (MMP-2), 9 (MMP-9), tissue inhibitor of metalloproteinase 1 (TIMP-1) and TIMP-2 in WT and gp91$^{phox-/-}$ mice determined by western blot. *p< 0.05 vs. respective control.

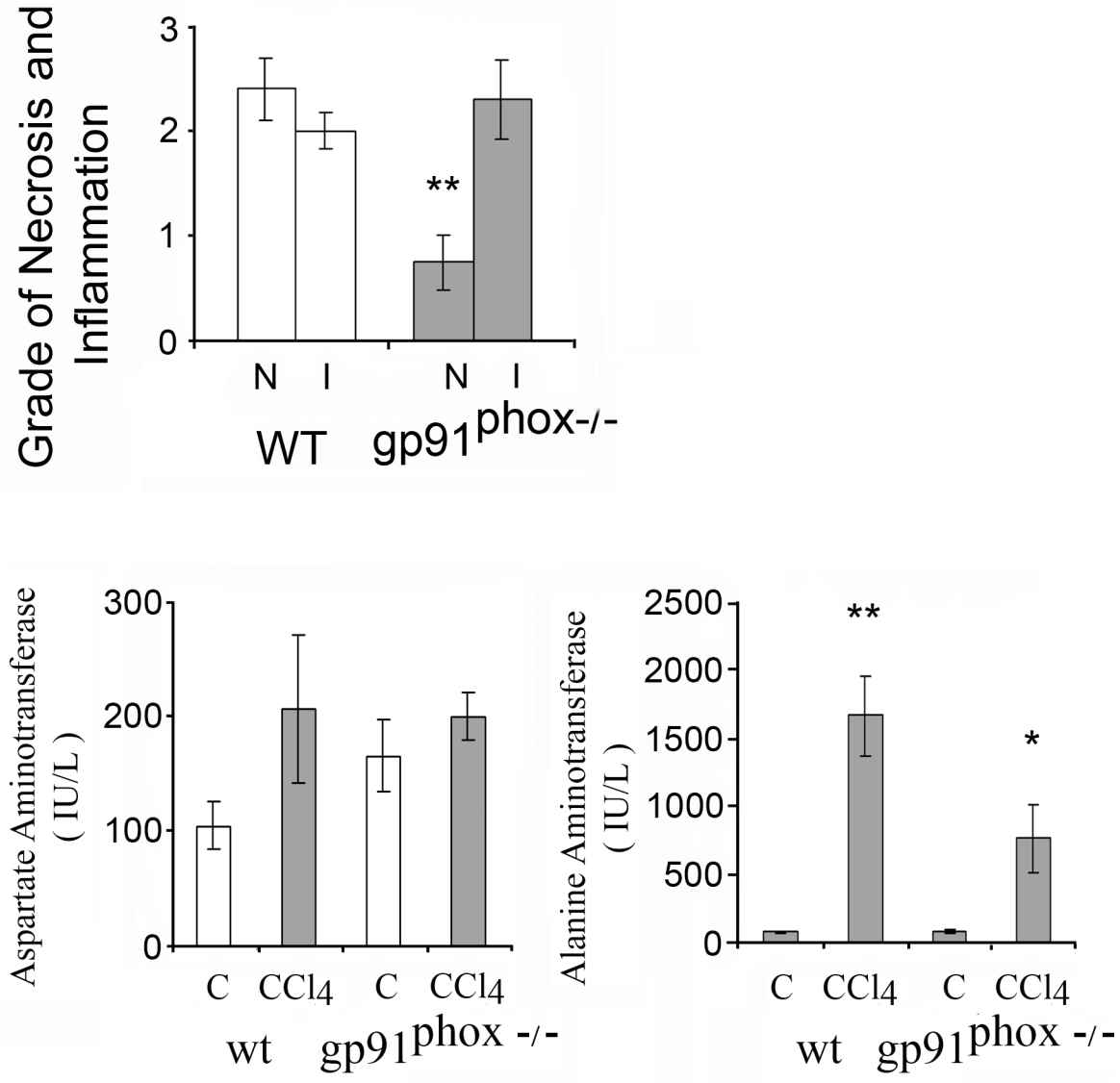

Fig. 8.

Necroinflammatory changes and serum aminotransferases after 1 week of CCl_4 administration in wild type (WT) and gp91$^{phox-/-}$ mice. Liver cell necrosis (N) was evaluated on a scale of 1–4 as follows: 1, occasional; 2, mild scattered; 3, confluent zonal and 4, extensive. Grades for hepatic inflammation (I) were: 1, scattered; 2, mild; 3, moderate and 4, marked. The histological changes were assessed in x 20 magnification fields of slides stained with hematoxylin-eosin (H&E). The values are expressed as means ± SE of 8 determinations per group. **p<0.01 vs. WT for necroinflammatory changes. *p<0.05 and **p<0.01 vs. control for serum aminotransferases.

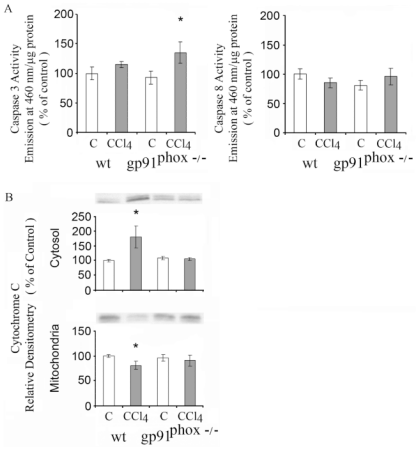

Fig. 9.

Effects of one week of chronic CCl_4 administration on A. Activities of caspase 3 and 8 and (B) on cytosolic and mitochondrial cytochrome c in WT and $gp91^{phox-/-}$ mice. Cytochrome c was determined by western blot and quantitated by densitometry. The values are expressed as means ± SE of of 8 measurements per group. * $p < 0.05$ vs. respective control.

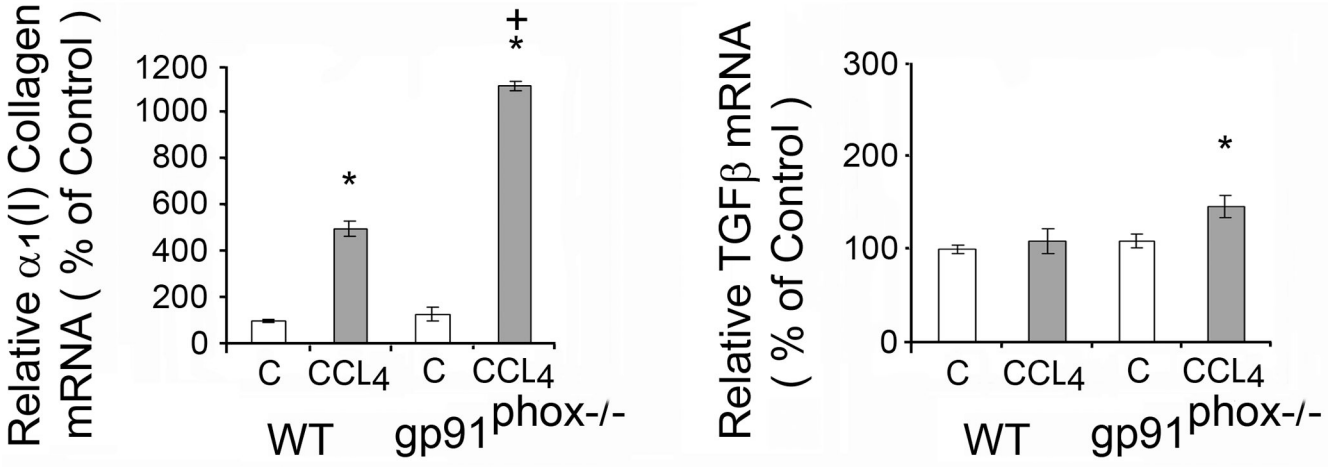

Fig. 10.

Liver α_1(I) collagen mRNA and transforming growth factor β (TGFβ) mRNA in WT and gp91$^{phox-/-}$ mice after one week of CCl_4 administration. The mRNAs were determined by real time quantitative PCR. The relative amounts of mRNA were normalized against β-actin in the same samples. The values are expressed as means ± SE. * $p < 0.05$ vs. respective control. $^{+}p<0.05$ vs. WT + CCl_4.

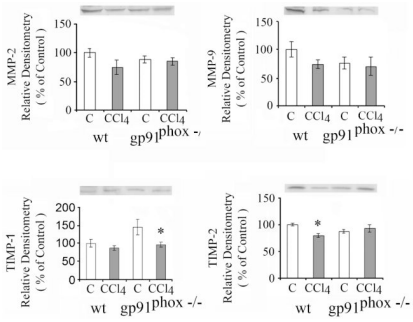

Fig. 11.

Effects of one week of CCl_4 administration on matrix metalloproteinase 2 (MMP-2), 9 (MMP-9), tissue inhibitor of metalloproteinase 1 (TIMP-1) and TIMP-2 in WT and $gp91^{phox-/-}$ mice determined by western blot. * $p < 0.05$ vs. respective control.

Table 1

Effects of carbon tetrachloride (CCl_4) administration for one week on matrix metalloproteinase-2 (MMP-2) mRNA, matrix metalloproteinase-8 (MMP-9) mRNA and tissue inhibitor of metalloproteinase 1 (TIMP-1) mRNA

mRNA	WT		gp91$^{phox-/-}$	
	Control	CCl_4	Control	CCl_4
MMP-2	100 ± 6.2	131 ± 3.7	107 ± 9.0	244 ± 45.1**
MMP-9	100 ± 8.3	148 ± 30.0	111 ± 9.6	198 ± 29.2*
TIMP-1	100 ± 12.1	33917 ± 77.6	124 ± 22.9	46469 ± 909^{**+}

The mRNAs were determined by real time quantitative PCR. The relative amounts of mRNA were normalized against β-actin in the same samples and expressed as a % of WT control for each determination. The values are expressed as means ± SE of 8 determinations per group.

* $p<0.05$ vs. control.

** $p<0.01$ vs. control.

$^{+}$ $p<0.05$ vs. WT + CCl4.